Multidecadal Variations of the Effects of the Quasi-Biennial Oscillation on the Climate System

Stefan Brönnimann[1,2], Abdul Malik[1,2], Alexander Stickler[1,2], Martin Wegmann[1,2], Christoph C. Raible[1,3], Stefan Muthers[1,3], Julien Anet[4], Eugene Rozanov[5,6], Werner Schmutz[6]

[1] Oeschger Centre for Climate Change Research, University of Bern, Switzerland

[2] Institute of Geography, University of Bern, Switzerland

[3] Climate and Environmental Physics, Physics Institute, University of Bern, Switzerland

[4] Swiss Federal Laboratories for Materials Science and Technology, Dübendorf, Switzerland

[5] Institute of Atmospheric and Climate Sciences, ETH Zurich, Switzerland

[6] PMOD/WRC Davos, Switzerland

Abstract

Effects of the Quasi-Biennial Oscillation (QBO) on tropospheric climate are not always strong or appear only intermittently. Studying them requires long time series of both the QBO and climate variables, which has restricted previous studies to the past 30-50 years. Here we use the benefits of an existing QBO reconstruction back to 1908. We first investigate additional, newly digitized historical observations of stratospheric winds to test the reconstruction. Then we use the QBO time series to analyze atmospheric data sets (reconstructions and reanalyses) as well as the results of coupled ocean-atmosphere-chemistry climate model simulations that were forced with the reconstructed QBO. We investigate effects related to (1) tropical-extratropical interaction in the stratosphere, wave-mean flow interaction, and subsequent downward propagation and (2) interaction between deep tropical convection and stratospheric flow. We generally find weak connections, though some are statistically significant over the 100-year period and consistent with model results. Apparent multidecadal variations in the connection between the QBO and the investigated climate responses are consistent with a small effect in the presence of large variability, with one exception: the imprint on the northern polar vortex, which is seen in recent reanalysis data, is not found in the period 1908-1957. Conversely, an imprint in Berlin surface air temperature is only found in 1908-1957, but not in the recent period. In the model simulations, likewise, both links tend to appear alternatingly, suggesting a more systematic modulation such as due to a shift in the circulation. Over the Pacific warm pool, we find increased convection during easterly QBO mainly in boreal winter in observation-based data as well as in the model simulations, with large variability. No QBO effects were found in the Indian monsoon strength or Atlantic hurricane frequency.

1. Introduction

The Quasi-Biennial Oscillation (QBO) is an oscillation of equatorial stratospheric zonal winds with a downward propagating phase taking approximately one year from the stratopause to the tropopause. It is relevant for interannual variability of stratospheric dynamics and composition (Baldwin et al., 2001), both in the tropics and the polar regions (e.g., Holton and Tan, 1980). The QBO also affects tropospheric weather, either through its effect on the stratospheric polar vortex (Baldwin et al., 2001) or perhaps directly through interaction with tropical convection (Collimore et al., 2003; Huang et al., 2012). Tropospheric imprints were found in the Eurasian region, including the North Atlantic or Arctic Oscillation and Eurasian snow cover (e.g., Peings et al., 2013). The QBO has also been claimed to affect the Indian monsoon system (e.g., Mukherjee et al., 1985), Atlantic hurricane frequency (Klotzbach, 2007) or El Niño/Southern Oscillation (Gray et al., 1992a,b).

Given the QBO's close-to-periodic variation (which implies predictability), any such mechanism raises hope to increase the prediction skill beyond the classical weather forecast of a couple of days (see Tripathi et al., 2015). Furthermore, the QBO might modulate forcing-response relationships. For instance, Labitzke et al. (2006) found that the QBO modulates the effect of solar activity on the polar vortex. Therefore, the QBO's effect on tropospheric climate is of interest to different areas of climate research.

Previous research has shown that the effects of the QBO on the troposphere are not always strong but appear only intermittently, e.g. between the 1950s and the 1980s (e.g., Camargo and Sobel, 2010). This calls for an analysis of long time series. The standard QBO time series - that of the Freie Universität Berlin (FUB) - reaches back to late 1953. Spectral analyses from earlier data confirm that the QBO existed before that time (Labitzke and van Loon, 1999). However, for the period prior to 1953, no direct comparison of stratospheric wind data and independent tropospheric climate data could so far be done, which is the aim of our paper. One starting point of our paper are historical studies pointing to a QBO imprint prior to 1953, which we here test with long data series and model simulations. In fact, a clear 2.2-yr cycle in Berlin surface air temperature (SAT) was already reported by Baur (1927). Landsberg (1962) and Landsberg et al. (1963) used spectral analysis of many more SAT series and found 2.2 yr cycles. Spectral analyses of the North Atlantic Oscillation (NAO) or the Northern Annular Mode indices also indicate significant peaks near 2.2 years (Hurrell and van Loon, 1997; Coughlin and Tung, 2001). More generally, speculations of a biennial oscillation in climate variables go back to the 19th century (see Clayton (1884, 1885) for precipitation and pressure in the United States, Woeikof (1895) for Scandinavian snow cover).

We base our analysis on a previous paper (Brönnimann et al., 2007), where we reconstructed the QBO back to 1908 by using the solar semidiurnal tide extracted from hourly sea-level pressure (SLP) data. The reconstruction was augmented by incorporating historical stratospheric wind observations and was validated using the QBO signature in historical total column ozone data. In the meantime, we have digitised a large amount of additional historical upper-air data (Stickler et al., 2014a), which partly cover the equatorial stratosphere. Among the new data are Berson's 1908 observations in East Africa (Brönnimann and Stickler, 2013), wind profiles from Batavia, 1910-1911, profiles from cruises of the research vessel Meteor 1925-1927 (Stickler et al., 2015), as well as several other measurements.

We first present the new data sources and compare the results to the previous reconstruction. After finding that the additional data do not contradict the previous reconstruction, we use the reconstruction to analyse the imprint of the QBO in observations-based data sets (historical reanalyses and reconstructions) of tropospheric circulation and climate. We analyse SAT, precipitation, snow cover, tropospheric wind fields, and hurricane tracks. The same analyses are performed in a set of four simulations with a coupled ocean-atmosphere-chemistry-climate model that were nudged to the same reconstructed QBO, but backwards extended to 1600, such that we have 4×405 years of model data available (Muthers et al., 2014).

The paper is organised as follows. In Section 2, we describe the historical upper-air data and the quality check of the QBO reconstruction and describe the climate model simulations. Results are presented in Section 3 and discussed in Section 4. Conclusions are drawn in Section 5.

2. Data and Methods

2.1. QBO time series

2.1.1. Historical evidence

Only sporadic information is available on the QBO before 1953. The first indirect indications of stratospheric wind variability relate to observations of volcanic plumes (Hamilton, 2012). The most famous example is the observation of the Krakatau volcanic plume in 1883, which circled the globe from east to west. The high altitude winds (the stratosphere was not yet discovered) responsible for this transport became widely known as "Krakatau easterlies".

Direct observations of equatorial stratospheric winds by means of balloons go back to 1908, when Berson, in an expedition to East Africa, reported unexpected westerly winds in the lower stratosphere (Süring, 1910). These westerlies were confirmed by van Bemmelen and Braak (1910), who performed observations of upper-level winds in Batavia from 1909 to

1918. Lower stratospheric westerlies were also confirmed by the observations of another volcanic eruption plume (Semeru, 15 Nov 1911) as reported by Hann and Süring (Hamilton, 2012). Reconciling Berson's westerlies with the expected easterly winds remained a challenge until the discovery of the QBO in the 1960s (Hastenrath, 2007).

Stratospheric wind observations were very sparse prior to the 1950s. The early results were summarized by Schove (1969) and Hamilton (1998). After the 1950s, when a global radiosonde network was built up, stratospheric winds were operationally observed in the equatorial region. It was in these data that Reed et al. (1961) and Veryard and Ebdon (1961) discovered the QBO. Based on radiosonde records from Canton Island (3° S, 172° W) from 1953 to 1967, Gan (Maledives, 1° S, 73° E) from 1967 to 1975 and Singapore (1° N, 104° E) since 1976, Naujokat (1986) and Marquardt and Naujokat (1997) were able to derive the QBO time series back to 1953, known as the FUB QBO. Since the advent of reanalysis data, the QBO is normally defined as the zonally averaged zonal wind in the stratosphere at the equator. We follow this definition.

2.1.2. Reconstruction of the QBO

In this paper we use the monthly reconstruction of the QBO (zonal mean zonal winds at the equator) from Brönnimann et al. (2007). This reconstruction is based on the surface signature of the QBO-modulated solar semidiurnal tide in hourly surface pressure observations from Batavia prior to 1945 as well as on historical upper-air wind profiles. For the reconstruction we first defined a perpetually repeating "ideal QBO cycle" from deseasonalized reanalysis data. Then we used the observational evidence to determine a time axis (i.e., timing of phases) and interpolated the ideal cycle onto this new time axis. Finally, we added back the annual cycle. We used historical total ozone data (which also show an imprint of the QBO) to assess the reconstruction and found generally good agreement, but the real QBO might be out of phase by up to 3 or 4 months.

The reconstruction is supported by historical upper-air observations mainly in the 1910s and in the 1940s, while the solar semidiurnal tide provides continuous information but stops in 1945, afterwards the reconstructions are entirely based on upper-air wind observations. The Freie Universität Berlin QBO starts in 1953. From September 1957 on, the QBO is taken from ERA-40 and after 1979 from ERA-Interim (Dee et al. 2011). The resulting 108-year QBO record is given in Fig. 1. We are currently in the 48th cycle since Berson's profile of 1908, which we take as a starting point of our work. The number of cycles thus allows robust statistics.

2.1.3. Additional historical upper-air data

The data presented here are part of a set of 1.25 million upper-air profiles that were digitised in the framework of the ERA-CLIM project (Stickler et al., 2014a,b), adding to the 12.75 million upper-air winds profiles that were already available from the Comprehensive Historical Upper-Air data set prior to 1957 (Stickler et al., 2010). A plot of most of the equatorial stratospheric data comprised in the latter data set was already given in Labitzke et al. (2006) and they entered the reconstruction described above. For this paper we collected all additional (ERA-CLIM) data prior to 1950 from stations within 20° S to 20° N. In the following we highlight three particular records.

2.1.3.1. Berson's East Africa Expedition

In 1908, the German meteorologist Arthur Berson organized an aerological expedition to East Africa with the aim to better understand the monsoon system (Fig. S1 shows the launch of a registering balloon on Lake Victoria). Upper-level winds were observed with pilot balloons and registering balloons (briefly described in Brönnimann and Stickler, 2013). Only few profiles reached the stratosphere. Surprisingly, some of them indicated westerly winds in the stratosphere. Figure S1 (right) shows the wind profiles that reached the stratosphere. Although all profiles except two were taken during an only 15-day interval, there is considerable scatter. It is very difficult to identify wind regimes from the raw data, although there are westerly winds in the stratosphere in several profiles.

The corresponding profiles from the reconstructions are also indicated. While there is a good agreement with some of the profiles (westerlies between 18 km and 20 km and easterlies above), others show relatively strong easterlies between 16 and 18 km (or even higher), where the reconstructions suggest zero zonal wind. Note that the reconstructions assumed westerly winds at 19 km altitude throughout the year 1908 based on the notion of Berson westerlies.

2.1.3.2. The Batavia data

In 1909 the Dutch Colonial Secretary started aerological observations in Batavia (van Bemmelen et al., 1911), supported by leading aerologists such as Richard Assmann and Hugo Hergesell. Kites, registering balloons and pilot balloons were used. Many of the balloons reached high altitudes, and soon westerlies winds were observed (van Bemmelen and Braak, 1910), thus confirming Berson's findings. Veryard and Ebdon (1961) and Ebdon (1963) analyzed the Batavia winds from 1909 to 1918 (which they published in the form of monthly

averaged wind directions for certain altitude bands) and found a clear QBO signature, including the downward phase propagation. Their published phases are interpretations, not raw data, and these phases were used to constrain our reconstructions. From the digitized data (Fig. S2 shows the earliest phase of measurements) it is however difficult to discern clear wind regimes.

2.1.3.3. Research vessel "Meteor"

From 1925 to 1927, the German research vessel Meteor cruised the Atlantic and took, in addition to many oceanographical measurements, also aerological observations. More than 1000 vertical profiles were retrieved on east-west transects across the tropical and South Atlantic (see Stickler et al., 2015 for details). Apart from kites and some registering balloon ascents (none of which reached the stratosphere), 801 pilot balloon ascents are available, of which the highest reached 20.5 km. In the tropical region (20°N to 20°S), however, only few measurements higher than 16 km are available.

These measurements (as well as those from Berson, Batavia and all other measurements from the ERA-CLIM data set) are incorporated as circles into Figure 1. Again it is difficult to find a coherent picture. Counting the agreement in sign of the zonal wind between observations and reconstructions, we find a rate of 60%. This is not a particularly good score for an evaluation, which is not even fully independent. The rate increases, though, if we only use observations above 19 or 20 km or exclude comparisons for which reconstructed winds are weak (i.e., close to phase change). Conversely, there is no systematic pattern of disagreement (no out-of-phase relation). We therefore continue and use our reconstructions for further analyses but note that the reconstruction remains to be further confirmed.

2.2. Atmospheric circulation and climate data

In order to analyse the imprint of the QBO in historical times, we use several data sets of the tropospheric circulation that cover the pre-1957 period. These data sets include the Twentieth Century Reanalysis (20CR; Compo et al., 2011), versions 2 and 2c, the reanalysis ERA-20C Deterministic (Poli et al., 2016) as well as several data sets based on reconstructions. An overview of the analysis periods and data sets used is given in Fig. S3. As a reference in the recent period we use the ERA-Interim reanalysis.

20CR is based on the assimilation of surface or SLP from the International Surface Pressure Data Bank (ISPD) and the International Comprehensive Ocean-Atmosphere Data Set (ICOADS), with monthly sea-surface temperatures (SSTs) and sea ice used as a boundary

condition. Versions 2 and 2c differ with respect to the ISPD versions used (v2 and v3.2.9, respectively), the starting year (1871 and 1851) and the SSTs used (HadISST1.1; Rayner et al., 2003, and SODAsi version 2; Giese et al., 2015, with the high latitudes (>60°) corrected to COBE-SST2; Hirahara et al., 2014). Previous validation studies have shown that 20CR agrees well with independent observations in the midlatitudes, but less so in the tropics. In this study we use the ensemble mean monthly mean data and focus on version 2c (20CRv2c).

The ERA-20C reanalysis reaches back to 1900 and uses very similar pressure input as 20CRv2c (ISPD version 3.2.6), but additionally also assimilates marine winds and uses a newer version of HadISST (HadISST2; see Poli et al., 2016). Results of ERA-20C and 20CRv2c are similar, and hence we show ERA-20C only where it deviates from 20CRv2c.

In addition to 20CRv2c we use monthly mean fields of wind and geopotential height (GPH) at different levels from a statistical reconstruction (Griesser et al., 2010), which reaches back to 1880. It is based on historical upper-air (after 1918) and surface data, which were calibrated against ERA-40 (Uppala et al., 2005) in a principal component regression approach. Here we use GPH at 100 hPa in the northern extratropics.

Further we also use monthly indices that were reconstructed based on surface and upper-level variables using regression approaches (Brönnimann et al., 2009; Zhou et al., 2009) calibrated against (and extended by) NCEP/NCAR Reanalysis (Kistler et al., 2001). The same indices were also calculated from 20CRv2c. Specifically, we use the indices Z100, defined as GPH difference between 75-90° N and 40-55° N at 100 hPa (Brönnimann et al., 2009) as a measure for the weakness of the polar vortex, the Pacific Walker Circulation index PWC (the difference in vertical velocity at 500 hPa between the areas [10°S–10°N, 180–100°W] and [10°S–10°N, 100–150°E] following Oort and Yienger (1996)), and the Dynamic Indian Monsoon Index DIMI (the difference in 850 hPa zonal wind between the areas [5–15°N, 40–80°E] and [20–30°N, 70–90°E] following Wang et al. 2001).

We further used GHCNv3 SAT from Berlin, a time series of Atlantic hurricane activity (Vecchi and Knutson, 2011) as well as the HadCRUT4v global SAT data set (Morice et al., 2012).

2.3. Climate model simulations

The reconstructed QBO, backward extended to 1600 by repeating the ideal QBO cycle plus seasonal cycle, was used to nudge the coupled chemistry-climate-ocean-atmosphere model SOCOL-MPIOM. The simulations are described in Muthers et al. (2014). In brief, SOCOL-MPIOM is a combination of the chemistry-climate model SOCOL version 3 (Stenke et al.,

1 2013), which is based on the middle atmosphere version of ECHAM5 (Roeckner et al., 2006;

2 Manzini et al., 2006) coupled to the chemical module MEZON (Model for Evaluation of

3 oZONe trends (Rozanov et al., 1999; Egorova et al., 2003), and the ocean model MPIOM

4 (Marsland, 2003; Jungclaus et al., 2006). The atmospheric model was run at a resolution of

5 T31 (approx. 3.75° × 3.75°), with 39 levels (model top at 0.01 hPa / 80 km). The vertical

6 resolution around the tropopause is 20-30 hPa (levels are at 69.6, 89.1, 113.3, 143.1, 179.6,

7 and 224.2 hPa). The ocean state in 1600 was branched off another simulation (Jungclaus et al.,

8 2010; see Muthers et al., 2014; Anet et al., 2014; for more details).

9 Four simulations were performed for the period 1600 to 2000. Two simulations, termed F13

10 and F14 (differing only in their initial state) use a relatively strong solar forcing while the two

11 simulations F23 and F24 (again differing only in their initial state) use a weaker solar forcing.

12 As will be shown later, no differences between the ensemble members are found with respect

13 to their QBO effects. We thus also analysed a sample in which the four simulations were

14 pooled.

15 Atmospheric circulation and climate indices are nearly uncorrelated between the model

16 simulations (strongest for DIMI, where one correlation between two simulations reached

17 0.14), while there is some correlation for Berlin temperature due to the common forced trend.

19 **2.5. Methods**

20 The following methodology is applied to all analyses. Target variables and fields are analysed

21 on a seasonal scale. Therefore, we first defined seasons that pertain to easterly or westerly

22 phases of the QBO. For testing those hypotheses that require interaction with the stratospheric

23 polar vortex and downward propagation, we defined the QBO phase from 50 hPa tropical

24 zonal mean wind in early winter (Nov.-Dec.) and then compared the climate records of the

25 late winter (Jan.-Mar; March for snow cover). Months close to the reconstructed phase change

26 (which is uncertain by up to 3-4 months) are excluded by requiring tropical zonal mean wind

27 at 50 hPa to exceed 5 m/s over a two months period (thus, although amplitude is not

28 accounted for directly, it enters through exclusion of weak winds). We chose these months

29 because interaction between the QBO and the polar vortex may occur in early winter. The

30 downward propagation from the polar stratosphere to the surface than takes several weeks and

31 the signal may persist in the troposphere.

32 For those hypotheses that involve direct interaction between the QBO and high-reaching

33 convection, we used the 70 hPa QBO in June-July (JJ), and November-December (ND) and

34 analysed the climate fields over a three months period starting with one month offset (JAS,

1   DJF, respectively). The JAS definition was preferred over the more classical JJA period

2   following Chattopadhyay and Bhatla (2002), who found a stronger QBO signature in the

3   Indian Monsoon in these months. The shorter lag (as compared to the polar vortex-based

4   analyses described above) allows a more direct adjustment of the tropospheric circulation to

5   stratospheric forcing. Periods when tropical zonal mean wind was weaker than 3 m/s were not

6   considered. Furthermore, for all analyses we excluded years following major tropical volcanic

7   eruptions (i.e., 1601, 1642, 1675, 1720, 1730, 1810, 1816, 1832, 1836, 1884, 1912, 1926,

8   1964, 1983, and 1992).

9   Note that for specific problems, more accurate definitions of seasons could be found (see

10   Gray et al., 1992a,b; Huang et al., 2012) at the price of simplicity or (possibly) independence.

11   When defined in the above way, we find 39 easterly and 43 westerly phases for the boreal

12   winter 50 hPa QBO since 1908. The corresponding numbers for the 70 hPa QBO for summer

13   (winter) are 26 (31) easterly and 36 (30) westerly phases. In FUPSOL at 50 hPa in winter

14   there are 162 westerly (118 easterly) phases, the corresponding numbers for 70 hPa phases in

15   summer (winter) are 165 (113) westerly and 108 (159) easterly phases, respectively.

16   Our main method is a composite analysis of the two phases (easterly minus westerly). The

17   difference of the mean values is tested using a heteroscedastic (unequal variance) t-test (Wilks,

18   2006). In the observation-based data we do this for the entire time period as well as for the

19   subperiods 1908-1957 and 1958-2012 (see also Roy (2014), for changes in tropospheric

20   signatures between the two periods). As a reference we also apply the composite analysis to

21   1979-2015 in ERA-Interim data. In the model we apply the method to the entire time period

22   for all simulations separately as well as for the pooled simulations. In the paper we show

23   composite fields only for the latter; corresponding composites for all ensemble members and

24   variables, including statistical significance, are shown in the Supplement. Finally, we also

25   performed 30-yr moving composites, both in the observation-based data and in the model

26   (only in the individual members). We then calculated standardized differences, by dividing

27   the difference in the 30-yr window by the standard deviation of the corresponding variable *x*,

28   s_x, over the entire period:

$$\Delta x_t = \frac{\dfrac{\sum_{t-\frac{1}{2}}^{t+\frac{1}{2}} x_t e_t}{\sum_{t-\frac{1}{2}}^{t+\frac{1}{2}} e_t} - \dfrac{\sum_{t-\frac{1}{2}}^{t+\frac{1}{2}} x_t w_t}{\sum_{t-\frac{1}{2}}^{t+\frac{1}{2}} w_t}}{s_x}$$

30

1   Where *l* is window length, *t* is time (years), and *e* and *w* are binary indicators of easterly and

2   westerly QBO phases, respectively. A window length of 30 years was chosen as this

3   represents the typical time period of data availability in many studies. However, as the effects

4   could be aliased by variability modes of a similar periodicity, we also tested other window

5   lengths (20 to 60 years) and found very similar results (not shown).

7   **3. Results and Discussion**

8   **3.1. QBO-polar vortex interaction and downward propagation**

9   **3.1.1 The QBO effect on the polar vortex and the NAO**

10   Several mechanisms responsible for QBO influence on tropospheric climate have been

11   proposed. One pathway, known as the Holton-Tan effect (Holton and Tan, 1980; Baldwin et

12   al., 2001), is through the extratropical stratosphere in boreal winter. This mechanism is

13   understood to operate via changes in the extratropical planetary wave activity flux. An

14   easterly QBO at 50 hPa leads to convergence of wave activity in the subtropical lower

15   stratosphere and in subpolar middle and upper stratosphere (e.g., Garfinkel et al., 2012). The

16   waves deposit easterly momentum and decelerate the mean flow. The signal can propagate

17   downward and eventually reach the Earth's surface, although the mechanism is still not fully

18   understood (see Anstey and Shepherd, 2014, Kidston et al. 2015; a review of the proposed

19   mechanisms is beyond the scope of this paper).

20   Compositing easterly minus westerly QBO in boreal winter in ERA-Interim since 1979 (Fig.

21   2) shows this classical response. The zonal mean zonal wind weakens, most strongly at

22   around 30 km, 70° N. Cooling is found above and warming below. GPH exhibits positive

23   anomalies poleward of 60° N in the lower stratosphere, indicative of a weak polar vortex. A

24   corresponding cross-section for 20CRv2c and ERA-20C (Fig S4) shows that, while ERA-20C

25   qualitatively reproduces the pattern found in ERA-Interim, 20CRv2c does not reproduce the

26   pattern in the stratosphere, but all data sets agree in the troposphere.

27   Reconstructions and reanalyses both do not provide reliable information for altitudes above

28   around 10-15 km. The highest level we analyse here is 100 hPa (note that this might be too

29   low to capture QBO effects but too high to be well reconstructed). In the Z100 index (Table

30   1) we find no significant effect in any of the subperiods. The early period even shows a

31   negative difference (thus opposite to what is expected from Fig. 2). A more consistent relation

32   is found within the model simulations, which is highly significant for the pooled sample and

33   is significant at the 95% (90%) level for 2 (3) out of the 4 simulations (Table 1).

Compositing 100 hPa GPH and 200 hPa zonal wind for January to March gives similar results (Fig. 3). The analysis of 20CRv2c (1908-2012) and of the simulations (ensemble mean) show almost opposite patterns, but it should be noted that there is hardly any significance in the 20CRv2c composites (Fig. S5; no significance at all is found in 100 hPa GPH). In order to test whether uncertainties in 20CRv2c in the early times could be the cause of that, we compared the composite for 100 hPa GPH for the 1908-1957 period between 20CRv2c, ERA-20C, and statistical reconstructions (Fig. S6). In fact, there are again some differences between the products. 20CRv2c exhibits a stronger negative signal over the polar region than the other data sets, but none shows the weakening of the vortex expected from the Holton-Tan effect.

The difference in the QBO imprint between the individual model simulations (Fig. S7) is smaller than between model and 20CRv2c analyses. Each of model simulations shows a significant signature over the polar region as well as between 35° and 45° N. The weakening of the zonal wind found in ERA-Interim in the recent period is reproduced qualitatively in the model simulations, but not in 20CRv2c.

The lack of a consistent signal in two subperiods could point to the lack of a signal in general or to an intermittent behaviour of the QBO signature. For instance, the base state of atmospheric circulation might have changed (e.g., Vecchi and Soden, 2007), which then modulates the QBO response either through change the amount of upward propagating wave avtivity, or its refraction. However, changes in wave activity diagnostics are debated even for more recent reanalysis products and are here deemed unusable for historical reanalyses.

The model results suggest that the QBO signal might be small (though significant), such that short periods may, by chance, show an opposite relation. To test this, East-West differences in 30-yr moving windows are analysed (Fig. 4). In fact, the standardized differences for such periods vary considerably in the model. In the observation-based data, the difference was largest for the interval 1960 to 1989, i.e., close to the time window in which the Holton-Tan effect was originally discovered (although the behaviour changed during the 1977-1997 period, see Lu et al. 2008). Note, however, that 20CRv2c shows a weaker signal than the other data sets also in the last period.

In all, the reconstructed QBO and polar vortex strength at 100 hPa from reconstructions and reanalysis prior to 1957 do not show a relation. This could be due to inferior data quality of either or a too low analysis level (note that ERA-Interim also does not show a significant response at that level (Table 1), but only at higher levels (Fig. 2)). The model does show a significant relation as expected from the Holton-Tan effect, but the signal is rather small or

1 transient. Results are consistent with ERA-Interim considering decadal variability as found in

2 the model.

3 To assess whether the QBO affects the surface the ERA-Interim analysis (Fig. 2) is again

4 consulted. Zonal averages indeed show small surface effects (weaker zonal wind, higher SAT

5 and pressure for easterly phases), but only poleward of 80 °N. Very often, the NAO index is

6 analysed as an indication for surface imprints of stratospheric perturbations. This index is well

7 constrained in 20CR (Compo et al. 2011) and hence the NAO index is treated similarly as

8 Z100. As expected, differences in the NAO have the opposite sign as those for Z100.

9 However, none of the differences in 20CRv2c are significant. In the model simulations,

10 differences are significant at the 90% level in one out of four simulations (the p-value for the

11 pooled sample is exactly 0.05). The 30-yr moving window composite of the NAO index

12 shows that the decadal variability of the difference is large (both in observations and model

13 simulations), but anti-correlated with that of Z100 (which is expected).

14 Perhaps the simple dipole-NAO index is not suitable to capture the response. We therefore

15 also analysed composites of SLP fields. We find negative anomalies at midlatitudes stretching

16 from the eastern North Atlantic to central Eurasia in both 20CRv2c and model simulations.

17 Indeed, the pattern is shifted southward as compared to a classical NAO pattern. In the North

18 Atlantic-European region, the agreement between model and observation-based data is

19 stronger at the surface than in the stratosphere (note that the pattern over North America, in

20 contrast, is almost opposite in 20CRv2c and model simulations). In the model, the signature is

21 consistent in all four simulations (Fig. S8). Thus, both the signatures in the stratosphere and in

22 SLP are consistent with the Holton-Tan effect, but the variability is so large that even with

23 very long records, results remain near the limit of significance.

25 **3.1.2. The QBO effect on surface air temperature in Eurasia**

26 Baur (1927) analysed the 100-yr record of Berlin SAT and found a very clear quasi-biennial

27 cycle. Within our QBO reconstructions, we also find highly significant differences for Berlin

28 SAT (we used observations rather than reanalyses) in winter (Jan.-Mar.) between East and

29 West phases of the QBO (50 hPa, Nov.-Dec.). SAT is higher during easterly phases of the

30 QBO. This is unexpected as Berlin SAT is positively correlated with the NAO and negatively

31 with Z100. The effect might be real as the model simulations (grid point 15° E, 50.1° N) also

32 show higher SAT during the easterly phase of the QBO as compared to the westerly phase,

33 albeit not significantly.

Interestingly, the difference is significant only in the first period (which is when Baur (1927) discovered 2.2-yr cyclicities in Berlin SAT) and over the entire period, but not in the post-1957 period. In other words, the difference was significant in the period when no effect in Z100 and NAO was found. The 30-yr moving windows difference in the model simulations shows a similar behaviour. There are multidecadal periods when the QBO signature in Berlin SAT is positive while the NAO (Z100) signature is around zero, and periods when the NAO signature is negative and that in Berlin SAT is around zero. As for the raw series, the 30-yr moving windows difference series of Berlin SAT, $-1 \times$ Z100, and NAO are positively correlated (numbers in Fig. 4). However, the curves do not scatter around the one-to-one line, as could be expected, but are slightly displaced towards the upper left quadrant (illustrated by their long-term average, as dots). A possible explanation for this behaviour is a dipole-like variation that is induced by the QBO, but the dipole structure itself shifts with changes in the background climate. The locations or indices considered then do not well capture the dipole structure anymore and do not show a strong signature. Part of the decadal variability in the QBO-surface climate relation might thus arise from decadal climatic variability such as latitudinal shifts of circulation features.

We analysed the effect of a possible change in the base state using standard circulation indices (such as the NAO itself, the Atlantic Multidecadal Oscillation or the Pacific Decadal Oscillation, all filtered with the same moving window), but did not find consistent results between model and observation-based analyses. In the 1940s, the subtropical jet was in a relatively poleward position and then retracted equatorward (Brönnimann et al. 2015). This might be a possible explanation, but further evidence for this is required.

The composite field of SAT based on 20CRv2c (HadCRUT4v shows similar results) reveals that the warming for easterly phases stretches across much of Eurasia. It seems well reproduced in the model simulations, where it maximizes between the Caspian and Aral Seas. However, there is quite a large discrepancy between individual simulations despite the fact that they are 405 years long (Fig. S9). For instance, the SAT signal over North America is totally different and results here are not robust.

Based on these results, we defined a new SAT index for the Caspian-Aral Sea region, which is the region with the strongest imprint in the model composites. Even in this optimized case, there are some (albeit few) 30-yr periods in the 4×405-yr model simulations that would exhibit a significantly negative relation when analysed in isolation.

3.1.3. The QBO effect on snow cover

Woeikof (1895) speculated that snow cover follows a biennial cycle. To test this, snow depth in March is analysed. The corresponding composites (see Fig. 3) are highly consistent with the results for SAT, but again do not show a systematic effect. The high-resolution snow cover product from ERA-20C shows very similar results as 20CRv2c (see Fig. S7), i.e., the QBO East minus West differences for the two subperiods differ, and they both differ from the model simulations.

From these analyses there is no indication that snow cover in March is affected by the QBO in a significant way. Conversely, we can also not exclude intermittent effects. Peings et al. (2013) found an effect of the QBO on Siberian snow cover, but only after 1976 and not before. Hence, Woeikof (1895) might still have captured a QBO signal when finding differences in snow cover in Scandinavian between even and odd years – or (what is more likely) he was picking up random variability.

3.2. QBO interaction with deep tropical convection

3.2.1. The QBO effect on the ENSO system and the Pacific Walker Circulation

In 1992, Gray et al. (1992a,b) suggested an effect of the QBO on the ENSO system. Later publications addressed the effect of the QBO on tropical convection in observations (e.g., Collimore et al., 2003; Huang et al., 2012; Liess and Geller, 2012) or models (e.g., Giorgetta et al., 1999; Garfinkel and Hartmann, 2011; Nie and Sobel, 2015). Several mechanisms have been suggested as to how a link might proceed. Giorgetta et al. (1999) found that wind shear near the tropopause associated to the QBO phase in the lowermost stratosphere affects deep convection in the warm pool area. Huang et al. (2012) argued that the change in static stability due to the temperature QBO might play a more important role. However, the role of clouds and other feedbacks is not well understood (e.g., Garfinkel and Hartmann, 2011).

According to the wind shear mechanism, lower shear would favour deeper convection. Climatologically, easterlies dominate over the warm pool in the uppermost troposphere, hence an easterly QBO phase at 70 hPa reduces the wind shear and would enhance convection. With respect to the temperature, a westerly QBO phase at 70 hPa is associated with warm layer below, leading to increased stability in the tropopause region and thus less convection. From both mechanisms we expect more convection during easterly phases of the QBO in the lower stratosphere. Therefore, stability and wind shear influences cannot easily be separated without more detailed diagnostics that are not available for our study.

The analysis in ERA-Interim (Fig. 5) for zonal averages over the Indonesian and the Pacific Warm Pool (120° E to 160° E) in boreal winter is consistent with the two suggested

mechanisms. While SAT and zonal wind do not show a tropospheric imprint, an increase in tropical convection is found for easterly phases. This increase is shifted towards the northern hemisphere relative to the climatological maximum in convection. It is statistically significant in the tropopause region.

As a first approach, we analysed the PWC index, which is well reconstructed and rather well constrained in 20CRv2c and ERA-20C (see Compo et al., 2011). We found no significant signature in observation-based data, but during the ERA-Interim period we find a significantly negative response (weakening Walker circulation during easterlies). In contrast, in the model the Walker circulation is stronger for easterly than for westerly QBO in both seasons (JAS and DJF), in some simulations highly significant. The latter is consistent with increased convection over the Pacific warm pool area (Fig. 5), the former is not.

This imprint can be better understood when analyzing fields rather than an index. Composites of SST, vertical velocity, and zonal winds at 10 m and at 200 hPa are shown in Figure 6 (see Fig. S12 for significance). The most obvious signature is a slight eastward shift of the centre of convection over Indonesia during easterly QBO phases, resulting in the pattern seen in ERA-Interim. This is seen in both seasons (though stronger in boreal winter) and it is also seen in observations and hence is robust. The response thus does not project well onto the Pacific Walker circulation and surface winds over the central Pacific remain unaffected. Note, however, that almost no areas show a significant response in 20CRv2c. Signatures in SST show a slight equatorial Pacific warming but a cooling in Indonesia. However, for these findings significance is also limited (see Fig. S10 and S11). The winter hemisphere subtropical jet moves poleward in 20CRv2c and to some extent also in the model simulations.

3.2.2. QBO effect on Atlantic hurricanes and on the Indian Summer Monsoon

Finally, we also briefly analysed the relation between the QBO and Atlantic hurricanes or the Indian Summer monsoon strength. In both cases, our results revealed no significant differences with the simple indices used. Note, however, that for the Indian summer monsoon the relation might be more complex (e.g., Claud and Terray, 2007). The existence of a Tropospheric Biennial Oscillation in the summer monsoon has been claimed (Meehl et al., 2003), but this might arise from white noise and not from deterministic processes (Stuecker et al., 2015).

4. Conclusions

1   Our analysis revealed relatively small influences of the QBO on the tropospheric climate,

2   which are however consistent with historical literature (which is not too surprising as the

3   underlying observation-based data are partly the same) and in some cases with climate model

4   simulations. Although issues of data quality also contribute in the case of observation-based

5   data, it is interesting that even with very long time series and very long model simulations,

6   only few statistically significant results are found. Multidecadal variations of QBO-climate

7   links are mostly consistent with a small signal in the presence of internal decadal climate

8   variability, although one of the results (the fact that periods with a QBO signatures in Berlin

9   surface temperature and in the NAO alternate) also points to possible climatic modulations.

10 Based on the analysis of 108 years of QBO and climate variables from reconstructions as well

11 as 4×405 years of data from climate model simulations, we thus conclude that:

12 (1) There is no evidence that the extended QBO reconstruction is out-of phase with the

13   true QBO, but further support for the reconstructions is clearly required.

14 (2) The relation between the QBO and climate variables is rather weak on average, but

15   characterized by large multidecadal fluctuations.

16 (3) In boreal winter, there are links between the QBO and the stratospheric polar vortex or

17   between the QBO and Berlin SAT, but the former relation is typically strong when the

18   latter is weak and vice versa (both in model and observations), suggesting a climatic

19   origin of the decadal modulation (such as decadal latitudinal shifts of circulation). The

20   relation to a more broadly defined Eurasian SAT index is more stable.

21 (4) There is a weak but significant effect of the QBO on deep convection over the Pacific

22   Warm Pool, mainly in boreal winter (an eastward shift of convection during easterly

23   QBO in the lowermost stratosphere). Though significant, this change does not project

24   strongly onto the Pacific Walker circulation or ENSO.

25 (5) Our results are consistent with historical literature and also with the sequence of

26   discoveries of (quasi-)biennial imprints in weather and climate, as expected for

27   analyses of small effects embedded within strong variability.

Acknowledgements.
This paper is dedicated to Karin Labitzke, who made major contributions to the understanding of QBO effects on climate. The work was supported by the Swiss National Science Foundation under grant CRSII2-147659 (FUPSOL II) and the EC FP7 project ERA-CLIM2.

References

Anet, J. G., Muthers, S., Rozanov, E. V., Raible, C. C., Stenke, A., Shapiro, A. I., Brönnimann, S., Arfeuille, F., Brugnara, Y., Beer, J., Steinhilber, F., Schmutz, W., and Peter, T.: Impact of solar vs. volcanic activity variations on tropospheric temperatures and precipitation during the Dalton Minimum, Clim. Past 10, 921-938, doi:10.5194/cp-10-921-2014, 2014.

Anstey, J. A., and Shepherd, T. G.: High-latitude influence of the quasi-biennial oscillation. Q. J. R. Metoerol. Soc. 140, 1–21, 2014.

Baldwin, M. P. and Dunkerton T. J.: Stratospheric harbingers of anomalous weather regimes, Science, 294, 581–584, 2001.

Baldwin, M. P., Gray, L. J. Dunkerton, T. J. Hamilton, K. Haynes, P. H. Randel, W. J. Holton, J. R. Alexander, M. J. Hirota, I. Horinouchi, T. Jones, D. B. A. Kinnersley, J. S. Marquardt, C. Sato, K. and Takahashi, M.: The Quasi-Biennial Oscillation, Rev. Geophys., 39, 179–229, 2001.

Baur, F.: Das Periodiogramm hundertjähriger Temperaturbeobachtungen in Berlin (Innenstadt). Meteorol. Z., 44, 414-418, 1927.

Braak, C.: Koninklijk Magnetisch en Meteorologisch Observatorium te Batavia, Verhandelingen No. 3, Drachen-, Freiballon- und Fesselballon-beobachtungen. Javasche Boekhandel en Drukkerij, Batavia, 1915.

Brönnimann S., Annis, J. L., Vogler, C., and Jones, P. D.: Reconstructing the quasi-biennial oscillation back to the early 1900s, Geophys. Res. Lett., 34, L22805, 2007

Brönnimann, S. and Stickler, A.: Aerological observations in the Tropics in the Early Twentieth Century, Meteorol. Z., 22, 349–358, 2013.

Brönnimann, S., Stickler, A., Griesser, T., Fischer, A. M., Grant, A., Ewen, T., Zhou, T., Schraner, M., Rozanov, E., and Peter T.: Variability of large-scale atmospheric circulation indices for the Northern Hemisphere during the past 100 years, Meteorol. Z., 18, 379–396, 2009.

Brönnimann, S., Fischer, A. M., Rozanov, E., Poli, P., Compo, G. P., and Sardeshmukh P. D.: Southward shift of the Northern tropical belt from 1945 to 1980. Nature Geoscience 8, 969-974, 2015.

Camargo, S. J., and Sobel, A. H.: Revisiting the influence of the quasi-biennial oscillation on tropical cyclone activity, J. Clim., 23, 5810–5825, doi:10.1175/2010JCLI3575.1, 2010.

Chattopadhyay, J. and Bhatla, R.: Possible influence of QBO on teleconnections relating Indian summer monsoon rainfall and sea-surface temperature anomalies across the equatorial pacific. Int. J. Climatol., 22, 121–127, 2002.

Claud, C., and Terray, P.: Revisiting the possible links between the quasi-biennial oscillation and the Indian summer monsoon using NCEP R-2 and CMAP fields, J. Clim., 20, 773–787, 2007.

Clayton, H. H.: A lately discovered meteorological cycle, Amer. Met. Journal 1, 130-144, 1884.

Clayton, H. H.: A lately discovered meteorological cycle, II, Amer. Met. Journal 1, 528-534, 1885.

Collimore C. C., Martin, D. W., Hitchman, M. H., Huesmann, A., and Waliser, D. E.: On The Relationship between the QBO and Tropical Deep Convection, J. Clim., 16, 2552-2568, 2003.

Compo, G. P., Whitaker, J. S., Sardeshmukh, P. D., Matsui, N., Allan, R. J., Yin, X., Gleason, B. E., Vose, R. S., Rutledge, G., Bessemoulin, P., Brönnimann, S., Brunet, M., Crouthamel, R. I., 1035 Grant, A. N., Groisman, P. Y., Jones, P. D., Kruk, M. C., Kruger, A. C., Marshall, G. J., Maugeri, M., Mok, H. Y., Nordli, Ø., Ross, T. F., Trigo, R. M., Wang, X. L., Woodruff, S. D., and Worley, S. J.: The Twentieth Century Reanalysis Project, Q. J. Roy. Meteor. Soc., 137, 1–28, 2011.

Coughlin, K., and Tung, K.-K.: QBO Signal found at the Extratropical Surface through Northern Annular Modes, Geophys. Res. Lett. 28, 4563-4566, doi:10.1029/2001GL013565, 2001

Dee, D. P., Uppala, S. M., Simmons, A. J., Berrisford, P., Poli, P., Kobayashi, S., Andrae, U., Balmaseda, M. A., Balsamo, G., Bauer, P., Bechtold, P., Beljaars, A. C. M., van de Berg, L., Bidlot, J., Bormann, N., Delsol, C., Dragani, R., Fuentes, M., Geer, A. J., Haimberger, L., Healy, S. B., Hersbach, H., Hólm, E. V., Isaksen, L., Kållberg, P., Köhler, M., Matricardi, M., McNally, A. P., Monge-Sanz, B. M., Morcrette, J.-J., Park, B.-K., Peubey, C., de Rosnay, P., Tavolato, C., Thépaut, J.-N. and Vitart, F.: The ERA-Interim reanalysis: configuration and performance of the data assimilation system, Q. J. R. Meteorol. Soc., 137, 553–597. doi: 10.1002/qj.828, 2011.

Ebdon, R. A.: The tropical stratospheric wind fluctuation: Evidence of its permanency from earlier data, Weather, 18, 2–7, 1963.

Egorova, T., Rozanov, E., Zubov, V., and Karol, I. L.: Model for investigating Ozone trends (MEZON), Izv. Atmos. Oceanic Phys.,39, 277–292, 2003.

Garfinkel, C. I., Shaw, T. A., Hartmann, D. L., and Waugh, D. W.: Does the Holton–Tan Mechanism Explain How the Quasi-Biennial Oscillation Modulates the Arctic Polar Vortex?. J. Atmos. Sci., 69, 1713–1733, 2012.

Garfinkel, C. I. and Hartmann, D. L.: The Influence of the Quasi-Biennial Oscillation on the Troposphere in Winter in a Hierarchy of Models. Part II: Perpetual Winter WACCM Runs. J. Clim. 68, 2026-2041, 2011

Giese, B. S., Seidel, H. F., Compo, G. P., and Sardeshmukh, P. D.: An ensemble of historical ocean reanalyses with sparse observational input (submitted), 2015.

Giorgetta, M. A., Bengtsson, L., and Arpe, K.: An investigation of QBO signals in the east Asian and Indian monsoon in GCM experiments, Clim. Dynam., 15, 435–450, 1999.

Gray, W. M., Sheaffer, J. D., and Knaff, J. A.: Hypothesized mechanism for stratospheric QBO influence on ENSO variability, Gophys. Res. Lett., 19, 107-110, 1992.

Gray, W. M., Sheaffer, J. D., and Knaff, J. A.: Influence of the stratospheric QBO on ENSO variability, J. Meteorol. Soc. Jpn., 70, 975-987, 1992.

Griesser, T., Brönnimann, S., Grant, A., Ewen, T., Stickler, A., and Comeaux, J.: Reconstruction of Global Monthly Upper-Level Temperature and Geopotential Height Fields Back to 1880, J. Clim., 23, 5590–5609, 2010.

Hamilton, K.: Quasi-biennial and other long period variations in the solar semidiurnal barometric oscillation: Observations, theory and a possible application to the problem of monitoring changes in global ozone, J. Atmos. Sci., 40, 2432–2443, 1983.

Hamilton, K.: Sereno Bishop, Rollo Russell, Bishop's Ring and the discovery of the "Krakatoa Easterlies". Atmos. Ocean, 50, 169–175, 2012.

Hamilton, K.: Observations of tropical stratospheric winds before World War II, Bull. Am. Meteorol. Soc., 79, 1367–1371, 1998.

Hastenrath, S.: Equatorial zonal circulations: Historical perspectives, Dynamics of Atmospheres and Oceans 43, 16-24, 2007.

Hirahara, S., Ishii, M. and Fukuda, Y.: Centennial-Scale Sea Surface Temperature Analysis and Its Uncertainty, J. Climate 27, 57-75, 2014.

Holton, J. R., and Tan, H. C.: The influence of the equatorial Quasi-Biennial Oscillation on the global circulation at 50 mb, J. Atmos. Sci., 37, 2200–2208, 1980.

Huang, B., Hu, Z.-Z. Kinter III, J. L., Wu, Z., and Kumar, A.: Connection of stratospheric QBO with global atmospheric general circulation and tropical SST. Part I: Methodology and composite life cycle, Climate Dyn., 38, 1–23, doi:10.1007/s00382-011-1250-7, 2012.

Hurrell, J. W. and van Loon, H.: Decadal variations in climate associated with the North Atlantic Oscillation, Climatic Change, 36, 301-326, 1997.

Jungclaus, J. H., Keenlyside, N., Botzet, M., Haak, H., Luo, J.-J., Latif, M., Marotzke, J., Mikolajewicz, U., and Roeckner, E.: Ocean circulation and tropical variability in the coupled model ECHAM5/MPI-OM, J. Clim., 19, 3952–3972, doi:10.1175/JCLI3827.1, 2006.

Kidston, J., Scaife, A. A., Hardiman, S. C., Mitchell, D. M., Butchart, N., Baldwin, M. P., and Gray, L. J.: Stratospheric influence on tropospheric jet streams, storm tracks and surface weather. Nat. Geosc., 8, 433–440, 2015.

Kistler, R., Kalnay, E., Collins, W., et al.: The NCEP-NCAR 50-year reanalysis: Monthly means CD-ROM and documentation, Bull. Am. Meteorol. Soc., 82, 247–267, 2001.

Klotzbach, P. J.: Revised Prediction of Seasonal Atlantic Basin Tropical Cyclone Activity from 1 August. Wea. Forecasting, 22, 937–949, 2007.

Labitzke, K., Kunze, M., Brönnimann, S.: Sunspots, the QBO and the stratosphere in the North Polar Region–20 years later, Meteorol. Z., 15, 355–363, 2006.

Labitzke, K., van Loon, H.: The stratosphere: Phenomena, history, and relevance, Springer, 1999.

Landsberg, H. E.: Biennial Pulses in the Atmosphere. Beitr. Phys. Atmos., 35, 184-194, 1962.

Landsberg, H. E., Mitchell Jr., J. M., Cruther, H. L., Quinlan, F. T.: Surface signs of the biennial atmospheric pulse. Mon. Wea. Rev., 91, 549-556, 1963.

Liess, S., and Geller, M. A.: On the relationship between QBO and distribution of tropical deep convection, J. Geophys. Res., 117, D03108, doi:10.1029/2011JD016317, 2012.

Lu, H., Baldwin, M. P., Gray, L. J., and Jarvis, M. J.: Decadal-scale changes in the effect of the QBO on the northern stratospheric polar vortex, J. Geophys. Res., 113, D10114, 2008.

Manzini, E., Giorgetta, M. A., Esch, M., Kornblueh, L., and Roeckner, E.: The influence of sea surface temperatures on the northern winter stratosphere: Ensemble simulations with the MAECHAM5 Model, J. Clim., 19, 3863–3881, doi:10.1175/JCLI3826.1, 2006.

Marsland, S.: The Max-Planck-Institute global ocean/sea ice model with orthogonal curvilinear coordinates, Ocean. Model., 5, 91–127, doi:10.1016/S1463-5003(02)00015-X, 2003.

Marquardt, C. and Naujokat, B.: An update of the equatorial QBO and its variability, SPARC Melbourne, WMO/TD-NO. 814, 87-90, 1997.

Meehl, G. A., Arblaster, J., Loschnigg, J.: Coupled ocean-atmosphere dynamical processes in the tropical Indian and Pacific oceans and the TBO, J. Clim., 16, 2138–2158, doi:10.1175/2767.1, 2003.

Morice, C. P., Kennedy, J. J., Rayner, N. A., Jones, P. D.: Quantifying uncertainties in global and regional temperature change using an ensemble of observational estimates: The HadCRUT4 data set, J. Geophys. Res. 117, D08101, 2012.

1 Mukherjee, B. K., Indira, K., Reddy, R. S., and Ramana Murty, B. V.: Quasi-Biennial
2   Oscillation in stratospheric zonal wind and Indian Summer Monsoon, Mon. Wea. Rev.,
3   113, 1421-1424, 1985.

4 Muthers, S., Anet, J. G., Stenke, A., Raible, C. C., Rozanov, E., Brönnimann, S., Peter, T.,
5   Arfeuille, F. X., Shapiro, A. I., Beer, J., Steinhilber, F., Brugnara, Y., and Schmutz, W.:
6   The coupled atmosphere–chemistry–ocean model SOCOL-MPIOM, Geosci. Model Dev.,
7   7, 2157-2179, 2014.

8 Naujokat, B: An update of the observed quasi-biennial oscillation of the stratospheric winds
9   over the tropics, J. Atmos. Sci., 43, 1873-1877, 1986.

10 Nie J., and Sobel, A. H.: Responses of Tropical Deep Convection to the QBO: Cloud-
11   Resolving Simulations, J. Atmos. Sci., 72, 3625–3638, 2015.

12 Oort A. H., and Yienger, J. J.: Observed interannual variability in the Hadley Circulation and
13   its connection to ENSO, J. Clim., 9, 2751–2767, 1996.

14 Peings, Y., Brun, E., Mauvais, V., and Douville, H.: How stationary is the relationship
15   between Siberian snow and Arctic Oscillation over the 20th century? Geophys. Res. Lett.,
16   40, doi:10.1029/2012GL054083, 2013.

17 Poli, P., Hersbach, H., Dee, D. P., Berrisford, P., Simmons, A. J., Vitart, F., Laloyaux, P., Tan,
18   D. G. H., Peubey, C., Thépaut, J.-N., Trémolet, Y., Hólm, E. V., Bonavita, M., Isaksen, L.,
19   and Fisher, M.: ERA-20C: An atmospheric reanalysis of the 20th century, J. Clim.,
20   doi:10.1175/JCLI-D-15-0556.1, 2016.

21 Rayner, N. A., Parker, D. E., Horton, E. B., Folland, C. K., Alexander, L. V., Rowell, D. P.,
22   Kent, E. C. and Kaplan, A.: Global analyses of SST, sea ice and night marine air
23   temperature since the late nineteenth century, J. Geophys. Res. 108, 4407, 2003.

24 Reed, R. G., Campbell, W. J., Rasmussen, L. A., and Rogers, D. G.: Evidence of downward-
25   propagating annual wind reversal in the equatorial stratosphere. J. Geophys. Res., 66, 813-
26   818, 1961.

27 Roeckner, E., Brokopf, R., Esch, M., Giorgetta, M., Hagemann, S., Kornblueh, L., Manzini,
28   E., Schlese, U., and Schulzweida, U.: Sensitivity of simulated climate to horizontal and
29   vertical resolution in the ECHAM5 atmosphere model, J. Clim., 19, 3771–3791, 2006.

30 Rozanov, E., Schlesinger, M. E., Zubov, V., Yang, F., and Andronova, N. G.: The UIUC
31   three-dimensional stratospheric chemical transport model: Description and evaluation of
32   the simulated source gases and ozone, J. Geophys. Res.,104, 11,755–11,781, 1999.

33 Roy, I.: The role of the sun in atmosphere-ocean coupling. Int. J. Climatol., 34, 655-677, 2014.

34 Schove, D. J.: The biennial oscillation, tree rings and sunspots, Weather, 24, 390–397, 1969.

35 Stenke, A., Schraner, M., Rozanov, E., Egorova, T., Luo, B., and Peter, T.: The SOCOL
36   version 3.0 chemistry-climate model: description, evaluation, and implications from an
37   advanced transport algorithm, Geosci. Model Dev., 6, 1407-1427, doi:10.5194/gmd-6-
38   1407-2013, 2013b.

39 Stickler, A., Grant, A. N., Ewen, T., Ross, T. F., Vose, R. S., Comeaux, J., Bessemoulin, P.,
40   Jylhä, K., Adam, W. K., Jeannet, P., Nagurny, A., Sterin, A. M., Allan, R., Compo, G. P.,
41   Griesser, T., Brönnimann, S.: The comprehensive historical upper-air network. Bull. Amer.
42   Meteorol. Soc., 91, 741-751, 2010.

43 Stickler, A., Brönnimann, S., Jourdain, S., Roucaute, E., Sterin, A., Nikolaev, D., Valente, M.
44   A., Wartenburger, R., Hersbach, H., Ramella-Pralungo, L., and Dee, D.: Description of the
45   ERA-CLIM historical upper-air data, Earth Syst. Sci. Data, 6, 29-48, doi:10.5194/essd-6-
46   29-2014, 2014a.

Stickler, A., Brönnimann, S., Valente, M. A., Bethke, J., Sterin, A., Jourdain, S., Roucaute, E., Vasquez, M. V., Reyes, D. A., Guzman, J. G., Allan, R., and Dee, D.: ERA-CLIM: Historical Surface and Upper-Air Data for Future Reanalyses. B. Amer. Meteorol. Soc., 95, 1419–1430, 2014b.

Stickler, A., Storz, S., Jörg, C., Wartenburger, R., Hersbach, H., Compo, G. P., Poli, P., Dee, D., and Brönnimann, S.: Upper−air observations from the German Atlantic Expedition (1925-27) and comparison with the Twentieth Century and ERA−20C reanalyses. Meteorol. Z., 24, 525-544, 2015.

Stuecker, M. F., Timmermann, A., Yoon, J., and Jin, F.-F.: Tropospheric Biennial Oscillation (TBO) indistinguishable from white noise, Geophys. Res. Lett., 42, 7785–7791, 2015.

Süring R: A. Berson's Bericht ¨uber die aerologische Expedition des königlichen aeronautischen Observatoriums nach Ostafrika im Jahre 1908 (Report by A. Berson about the aerological expedition of the Royal Aeronautic Observatory to East Africa in 1908). Meteorol. Z., 27, 536–542, 1910 (translated and edited by Volken, E. and Brönnimann, S., Meteorol. Z., 22, 343-348, 2013).

Titchner, H. A., and Rayner, N. A.: The Met Office Hadley Centre sea ice and sea surface temperature data set, version 2: 1. Sea ice concentrations, J. Geophys. Res. 119, 2864-2889, 2014.

Tripathi, O. P., Baldwin, M., Charlton-Perez, A., Charron, M., Eckermann, S. D., Gerber, E., Harrison, R. G., Jackson, D. R., Kim, B.-M., Kuroda, Y., Lang, A., Mahmood, S., Mizuta, R., Roff, G., Sigmond, M. and Son, S.-W.: The predictability of the extratropical stratosphere on monthly time-scales and its impact on the skill of tropospheric forecasts, Q. J. R. Meteorol. Soc.. 141, 987-1003, doi: 10.1002/qj.2432, 2015.

Tung, K. K., and Yang, H.: Global QBO in circulation and ozone. Part I: Reexamination of observational evidence, J. Atmos. Sci., 51, 2699–2707, 1994.

Uppala, S. M., Kållberg, P. W., Simmons, A. J., Andrae, U., Bechtold, V. Da Costa, Fiorino, M., Gibson, J. K., Haseler, J., Hernandez, A., Kelly, G. A., Li, X., Onogi, K., Saarinen, S., Sokka, N., Allan, R. P., Andersson, E., Arpe, K., Balmaseda, M. A., Beljaars, A. C. M., Berg, L. Van De, Bidlot, J., Bormann, N., Caires, S., Chevallier, F., Dethof, A., Dragosavac, M., Fisher, M., Fuentes, M., Hagemann, S., Hólm, E., Hoskins, B. J., Isaksen, L., Janssen, P. A. E. M., Jenne, R., McNally, A. P., Mahfouf, J.-F., Morcrette, J.-J., Rayner, N. A., Saunders, R. W., Simon, P., Sterl, A., Trenberth, K. E., Untch, A., Vasiljevic, D., Viterbo, P., Woollen, J.: The ERA-40 re-analysis, Q. J. R. Meteorol. Soc., 131, 2961–3012, 2005.

van Bemmelen, and Braak, C.: Preliminary report upon the investigation of the upper air-layers begun at Batavia in 1909. Verh. K. Akad. Van Wetensch. te Amsterdam [Proceedings of the Royal Netherlands Academy of Arts and Sciences, Amsterdam] 13 I, 149-157, 1910.

van Bemmelen, W.: Die Wind-verhältnisse in den oberen Luftschichten nach Ballonvisierungen in Batavia. - Koninklijk Magnetisch en Meteorologisch Observatorium te Batavia. Verhandelingen No. 1, 1911.

van Bemmelen, W.: Koninklijk Magnetisch en Meteorologisch Observatorium te Batavia, Verhandelingen No. 4, Results of Registering-Balloon Ascents at Batavia. Javasche Boekhandel en Drukkerij, Batavia, 1916.

Vecchi, G. A., and Soden. B. J.: Global warming and the weakening of the tropical circulation. J. Climate, 20, 4316–4340, 2007.

Vecchi, G. A., and Knutson, T. R.: Estimating annual numbers of Atlantic hurricanes missing from the HURDAT database (1878-1965) using ship track density, J. Clim., 24, 1736–1746, 2011.

Veryard, R. G., and Ebdon, R. A.: Fluctuations in tropical stratospheric winds. The Meteorological magazine 90, 125–143, 1961.

Wang B., Wu R., and Lau K. M.: Interannual variability of the Asian summer monsoon: Contrasts between the Indian and the western North Pacific-East Asian monsoons, J. Clim. 14, 4073–4090, 2001.

Wilks, D. S.: Statistical methods in atmospheric sciences, 2nd Edition. Academic Press, 2006.

Woeikof, A.: Die Schneedecke in "paaren" und "unpaaren" Wintern, Meteorol. Z., 12, 77–78, 1895.

Zhou, T., Brönnimann, S., Griesser, T., Fischer, A. M., and Zou, L.: A reconstructed dynamic Indian monsoon index extended back to 1880, Clim. Dynam., 34, 573–585, 2010.

1 **Tables**

3 Table 1. Standardised difference in indices between easterly and westerly QBO phases in
4 different observation-based data sets as well as in the climate model simulations (F13, F14,
5 F23, and F24 denote the simulation numbers, also shown is the result for the pooled
6 simulations). Bold and italics denote significance at the 95% and 90% level, respectively.
7 REC+NNR is the combination of reconstructed indices up to 1947 and NCEP/NCAR
8 Reanalysis thereafter.

Index	1908-2014	1908-1957	1957-2014	1979-2015	F13	F14	F23	F24	Pooled
Z100 (REC+NNR)	0.226	-0.037	0.425	0.343	**0.304**	*0.206*	**0.279**	0.163	**0.238**
Z100 (20CRv2c)	-0.242	-0.443	-0.123	-0.184					
Z100 (ERA20C)	0.025	-0.057	0.162	0.206					
Z100 (ERA-Interim)				0.251					
NAO (20CRv2c)	0.088	0.356	-0.100	0.000	-0.002	*-0.213*	-0.183	-0.081	*-0.120*
Berlin Temp (GHCN)	**0.513**	**1.217**	0.015	0.116	*0.209*	-0.158	0.012	0.159	0.056
PWC$_{DJF}$ (REC+NNR)	0.049	0.004	-0.003	0.003	**0.280**	**0.340**	**0.367**	0.026	**0.253**
PWC$_{DJF}$ (20CRv2c)	0.111	0.002	0.002	0.015					
PWC$_{DJF}$ (ERA20C)	0.143	0.006	0.001	0.531					
PWC$_{JAS}$ (REC+NNR)	*-0.497*	-0.381	-0.676	**-1.406**	**0.356**	0.108	**0.235**	-0.127	**0.143**
PWC$_{JAS}$ (20CRv2c)	-0.289	-0.323	-0.254	**-1.300**					
PWC$_{JAS}$ (ERA20C)	-0.248	-0.239	-0.244	**-1.186**					
DIMI$_{JAS}$ (REC+NNR)	0.164	-0.239	0.713	0.520	-0.044	0.040	-0.091	0.005	-0.022
DIMI$_{JAS}$ (20CRv2c)	0.250	0.108	0.509	0.746					
DIMI$_{JAS}$ (ERA20C)	-0.187	-0.359	0.031	-0.461					
Hurricanes	-0.100	-0.016	-0.173	-0.674	NA	NA	NA	NA	NA

1 **Figures**
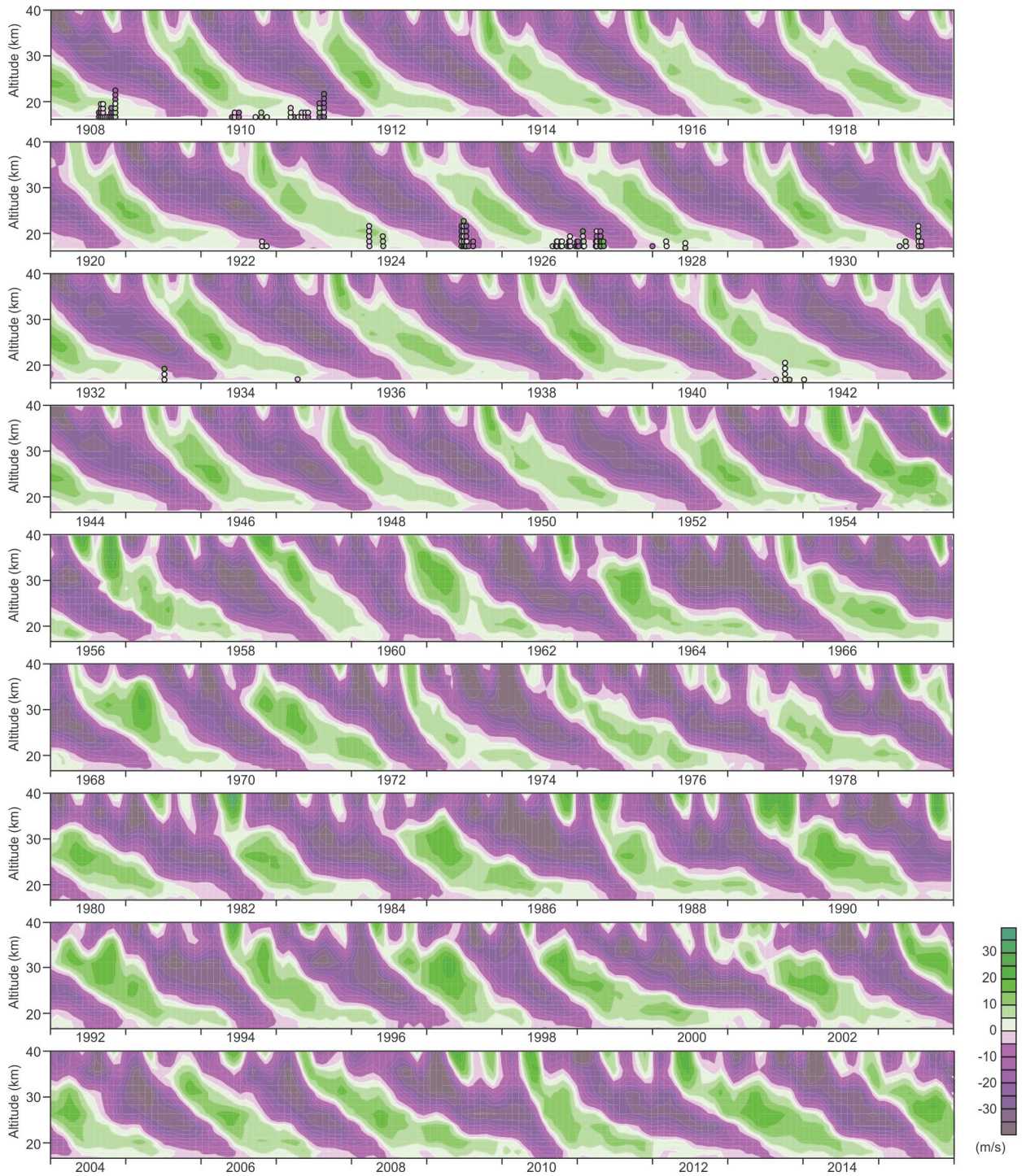
4 **Fig. 1.** Hovmöller diagram (time–height cross section) of zonal-mean zonal wind at the

5 equator from 1908 to 2015 (from Brönnimann et al., 2007). The dots in the first three rows

6 indicate the additional wind data rescued within the ERA-CLIM project.
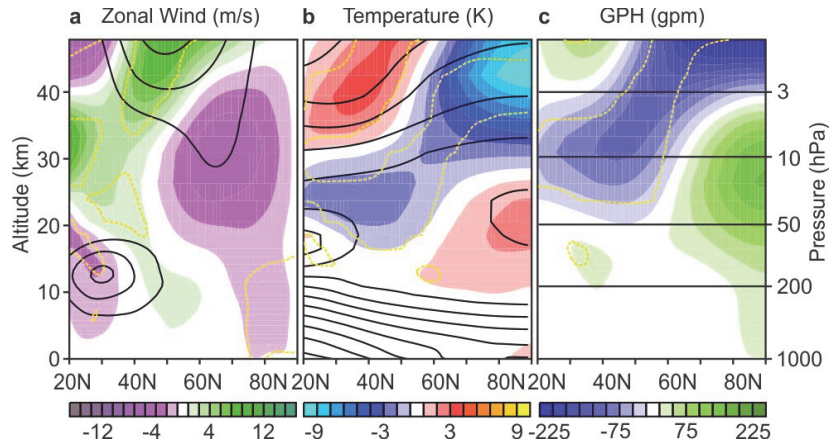
2 **Fig. 2.** Composite fields (shading) and climatologies (contours) since 1979 in ERA-Interim,

3 Jan.-Mar., for easterly minus westerly QBO phases (Nov.-Dec.) for zonal averages of (a)

4 zonal wind (contours: 20 to 60 m/s in steps of 10 m/s), (b) temperature (contours: 200 to 300

5 K in steps of 10 K) and (c) GPH. Yellow dashed lines indicate significant differences (p =

6 0.05). The corresponding figures for 20CRv2c and ERA-20C are given in Fig. S4.
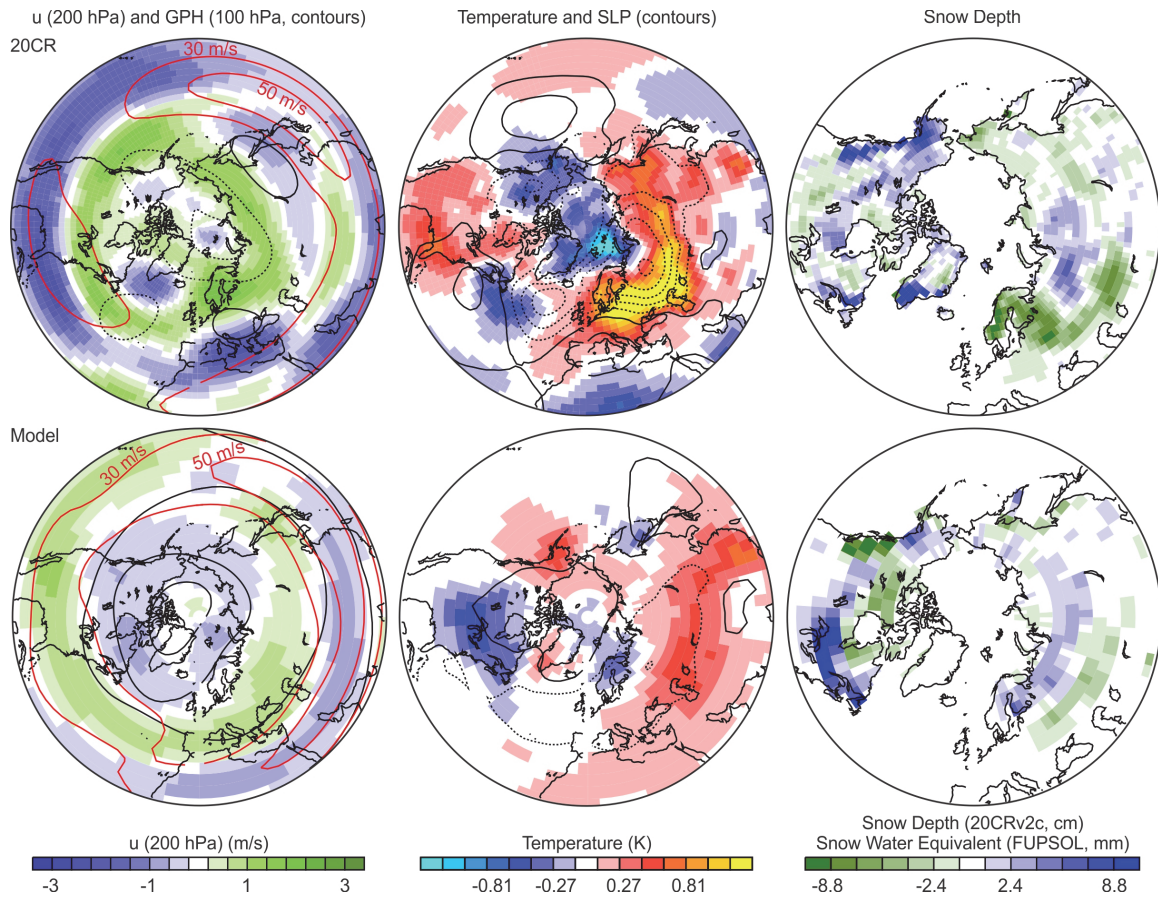
Fig. 3. Composite fields for easterly minus westerly QBO phases for (left) 200 hPa zonal wind (shading, red contours indicate climatology) and 100 hPa GPH (black contours, spacing 24 gpm, symmetric around zero, dashed are negative), (middle) surface air temperature (shading) and SLP (contours, spacing 0.6 hPa, symmetric around zero, dashed are negative) and (right) snow cover. See Fig. S5 for significance.
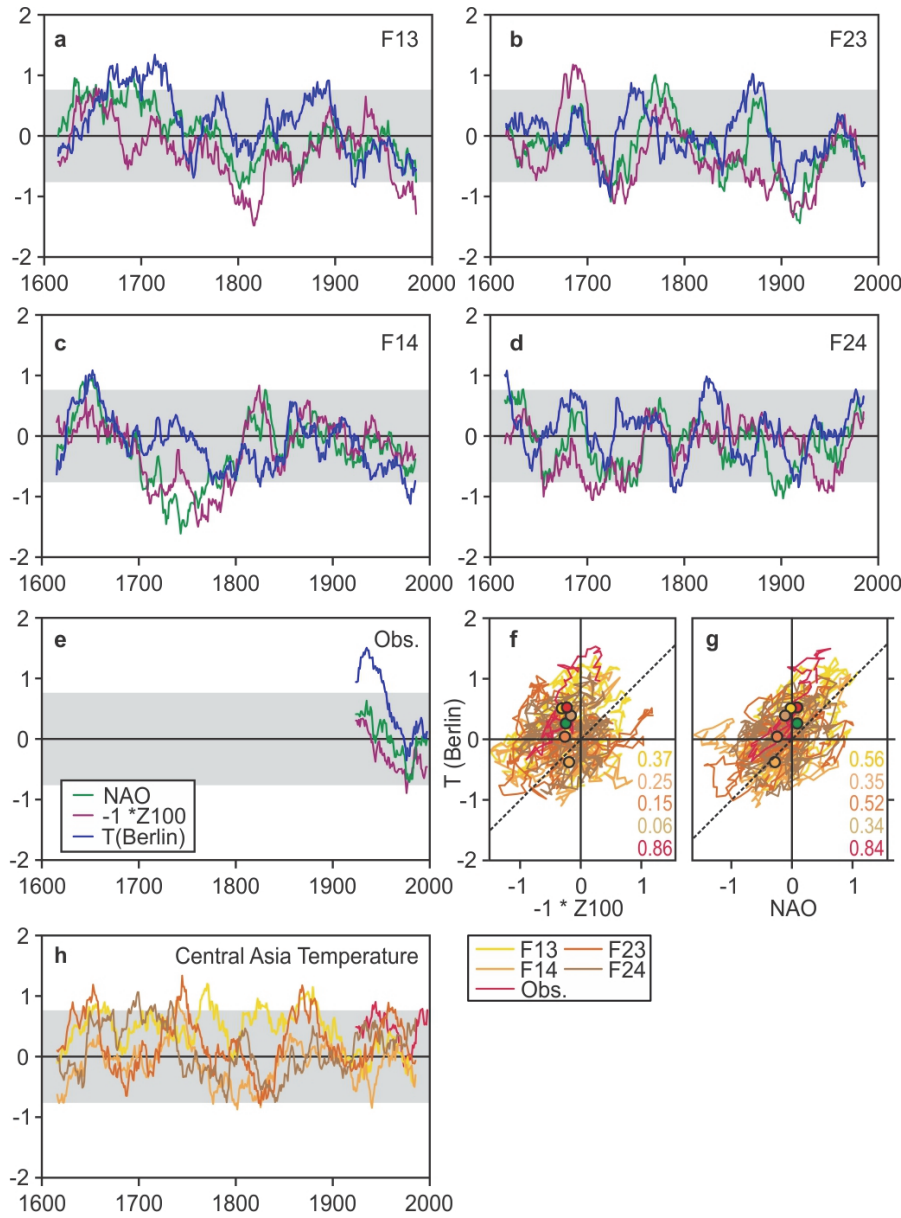
Fig. 4. Standardized differences between easterly and westerly QBO phases in 30-yr moving windows for NAO, Z100 and Berlin SAT in the four model simulations (a) F13, (b) F14, (c) F23, and (d) F24) and in (e) observation-based data (Z100 from reconstructions, NAO from 20CRv2c). Panels (f) and (g) show the same time series, but plotting Berlin SAT as a function of -1 * Z100 or NAO (filled circles indicate the standardized difference over the entire period and numbers give the correlations; the green circles indicates the standardized differences from ERA-Interim, 1979-2015, one-to-one lines are given in dashed). Panel (h) shows standardized differences between easterly minus westerly QBO phases in 30-yr moving windows for the Central Asia SAT index in HadCRUT4v and in the model simulations. Grey shading denotes an approximate 95% confidence interval for 30-yr averages.
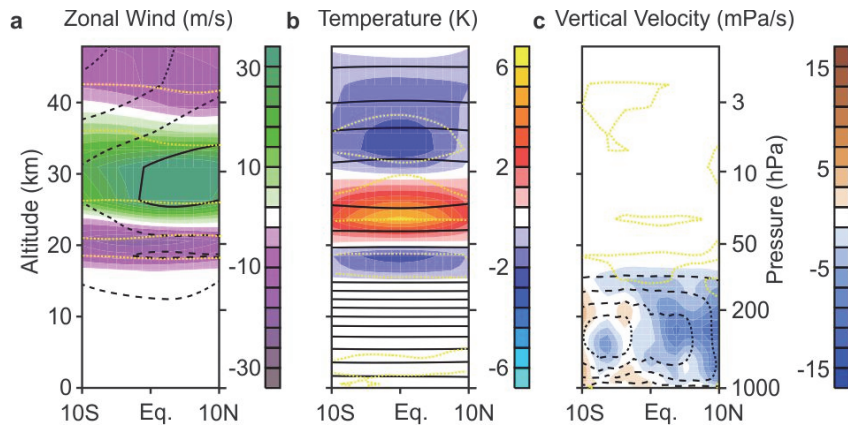
4   **Fig. 5.** Composite fields (shading) and climatologies (contours) of ERA-Interim for boreal

5   winter for easterly minus westerly QBO phases for zonal averages within 120-160° E for (a)

6   zonal wind contours: (-50 to 50 m/s in steps of 20 m/s), (b) temperature (contours: 200 to 300

7   K in steps of 10 K) and (c) omega (-70 to 70 Pa/s in steps of 20 Pa/s) in Dec.-Feb. using the

8   70 hPa QBO definition. Yellow dashed lines indicate significant difference (p = 0.05).
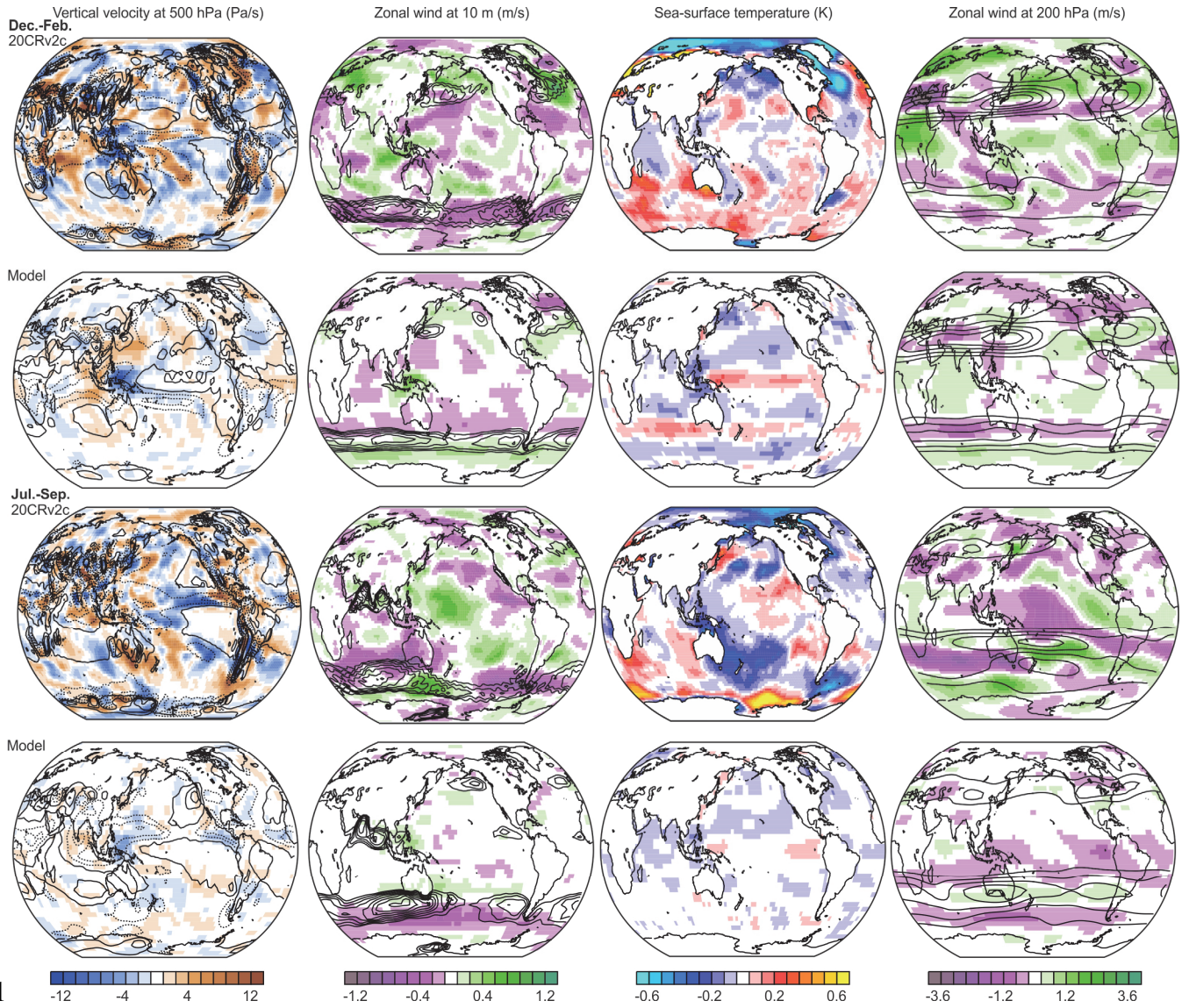
3 **Fig. 6.** Composite fields for easterly minus westerly QBO phases for (left) 500 hPa vertical

4 velocity (shading, contours indicate climatology, spacing is 40 Pa/s symmetric around zero,

5 dashed are negative), 10 m zonal wind (shading, contours indicate climatology from 4 m/s in

6 steps of 1 m/s), SST, and 200 hPa zonal wind (shading, contours indicate climatology from 20

7 m/s in steps of 10 m/s) for boreal summer and winter in 20CRv2c and in the model

8 simulations. See Fig. S12 for significance.